Magnetic properties of sintered $Sm_2Fe_{17}N_y$ magnets

Bo-Ping Hu, Xiao-Lei Rao, Jian-Min Xu, Gui-Chuan Liu, Yi-Zhong Wang, and Xiao-Lin Dong
San Huan Research Laboratory, Chinese Academy of Sciences, P.O. Box 603, Beijing 100080, China

Deng-Xia Zhang and Ming Cai
Institute of Mechanics, Chinese Academy of Sciences, Beijing 100080, China

(Received 15 October 1992; accepted for publication 29 March 1993)

Sintered magnets of $Sm_2Fe_{17}N_y$ nitrides, with a density of 6.0–7.4 g/cm^3, have been prepared by using an explosion technique. Both crystalline structure and the magnetic properties of $Sm_2Fe_{17}N_y$ nitrides were retained in the process. The sintered magnet had a remanence B_r=0.83 T, an intrinsic coercivity $\mu_0 H_c$=0.57 T and an energy product $(BH)_{max}$=88 kJ/m^3. The temperature dependence of coercivity and remanence were also measured. The temperature coefficients α of remanence and β of coercivity are −0.076%/°C and −0.51%/°C, respectively.

I. INTRODUCTION

Since the discovery of the $R_2Fe_{17}N_y$ nitride by Coey and Sun in 1990,[1,2] much work has been reported both on its intrinsic magnetic properties[3–8] and hard magnetic properties.[9–11] Since it possesses very good intrinsic magnetic properties with a Curie temperature of 749 K and a room-temperature anisotropy field of 14 T, which is superior to $Nd_2Fe_{14}B$, and a room-temperature saturation magnetization of 1.5 T, the $Sm_2Fe_{17}N_y$ nitride is expected to become a new permanent magnet for applications. The $Sm_2Fe_{17}N_y$ nitride with an intrinsic coercivity $\mu_0 H_c$ of more than 4 T has been achieved by mechanical alloying.[12] The $Sm_2Fe_{17}N_y$ magnets bonded by metal zinc have intrinsic coercivities $\mu_0 H_c$ over 0.5 T and an energy product $(BH)_{max}$ about 80 kJ/m^3.[9,10] The $Sm_2Fe_{17}N_y$ magnet bonded by epoxy resin has a $\mu_0 H_c$ of 1.08 T and $(BH)_{max}$ of about 72 kJ/m^3.[11] Since the $Sm_2Fe_{17}N_y$ nitride decomposes at high temperature (>650 °C), the conventional powder metallurgy technique cannot be used for making the sintered $Sm_2Fe_{17}N_y$ permanent magnet. In order to overcome this difficulty, in our previous work we reported that the sintered $Sm_2Fe_{17}N_y$ magnet can be made by the explosion technique.[13] In this work, we studied the structural and magnetic properties of the sintered $Sm_2Fe_{17}N_y$ magnet in detail. The structural properties were investigated by scanning electron microscopy (SEM) and transmission electron microscopy (TEM). The coercivity mechanism will be discussed according to the temperature variation of coercivity. Also, the temperature coefficients α of B_r and β of $_iH_c$ will be compared with those of Nd-Fe-B magnets.

II. EXPERIMENTAL METHODS

The Sm_2Fe_{17} alloy was prepared by arc melting the elements with a purity of better than 99.5% with about a 30% excess of Sm for compensating the melting loss, and then annealed in vacuum at a temperature of 950–1050 °C for 5–10 h. The homogenized Sm_2Fe_{17} compound was pulverized into a fine powder with an average size of about 20 μm. The nitrogenation was performed by heating the Sm_2Fe_{17} powder in pure nitrogen gas at a temperature of about 500 °C for 2 h.

The $Sm_2Fe_{17}N_y$ fine powder with an average size from 3 to 5 μm was prepared by ball milling and then pressed to be a cylinder, 15 mm in diameter and 20 mm in length, in an applied field of about 1.5 T. The cylinder was sintered by the explosion technique. It was put in a closed small die, and then exploded out. Initiating the explosive, a high-pressure shock wave propagates along the axis direction of the cylinder at a very short time. At the same time, the cylinder was compacted to be a high-density magnet by the shock wave. The sintered magnet has a density of ρ=6.0–7.4 g/cm^3, which is above 80% of the theoretical value. Five samples were investigated:

(i) Sample A: average size of nitride powder $\langle\mu\rangle$=3 μm; density of sintered magnet ρ=6.5 g/cm^3.

(ii) Sample B: average size of nitride powder $\langle\mu\rangle$=3 μm; density of sintered magnet ρ=6.2 g/cm^3.

(iii) Sample C: average size of nitride powder $\langle\mu\rangle$=5 μm; density of sintered magnet ρ=6.8 g/cm^3.

(iv) Sample D: average size of nitride powder $\langle\mu\rangle$=3 μm; density of sintered magnet ρ=6.4 g/cm^3.

(v) Sample E: average size of nitride powder $\langle\mu\rangle$=1 μm; density of sintered magnet ρ=6.0 g/cm^3.

X-ray diffraction was used to check the phase purity. The Curie temperatures were measured using a vibrating sample magnetometer in an applied field of about 0.06 T. Demagnetization curves in an open circuit at room temperature were measured up to 1.2 T on an extracting sample magnetometer.

III. RESULTS AND DISCUSSION

A. Crystalline structure and magnetic properties (sample A)

The x-ray diffraction patterns show that both the Sm_2Fe_{17} alloy and $Sm_2Fe_{17}N_y$ nitride are single phases with a Th_2Zn_{17}-type structure [Figs. 1(a) and 1(b)]. The α-Fe impurity appears after ball milling [Fig. 1(c)] and increases a little more after explosion sintering [Fig. 1(d)]. It

 0021-8979/93/74(1)/489/6/$6.00 © 1993 American Institute of Physics

Downloaded 10 Nov 2009 to 159.226.231.70. Redistribution subject to AIP license or copyright; see http://jap.aip.org/jap/copyright.jsp

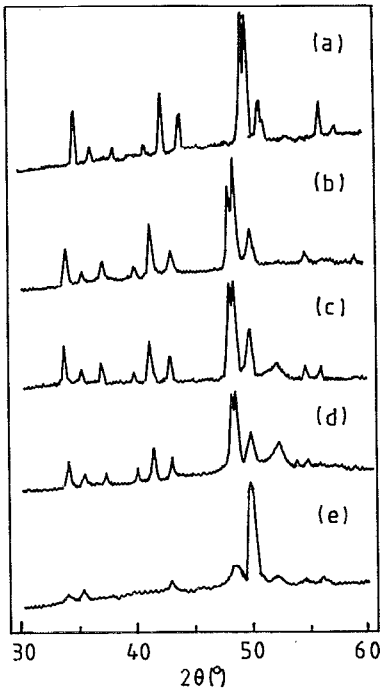

FIG. 1. X-ray diffraction patterns (Co$K\alpha$) of (a) Sm_2Fe_{17} alloy, (b) $Sm_2Fe_{17}N_y$ nitride powder, (c) $Sm_2Fe_{17}N_y$ nitride powder ball milled for 6 h, (d) powder of the explosion sintered $Sm_2Fe_{17}N_y$ magnet, and (e) on the orientation surface of the explosion sintered $Sm_2Fe_{17}N_y$ magnet.

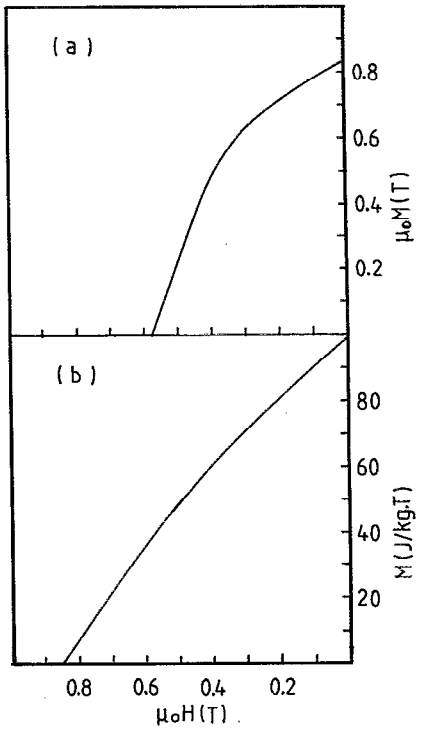

FIG. 3. Demagnetization curve of (a) explosion sintered $Sm_2Fe_{17}N_y$ magnet and (b) wax bonded magnet of $Sm_2Fe_{17}N_y$ ball milled for 6 h.

is clear that the explosion sintering does not change the crystalline structure of the $Sm_2Fe_{17}N_y$ nitride [Figs. 1(c) and 1(d)] or the alignment of the magnet [Fig. 1(e)].

Magnetization as a function of temperature in an applied field of 1.2 T is shown in Fig. 2. It can be seen that the

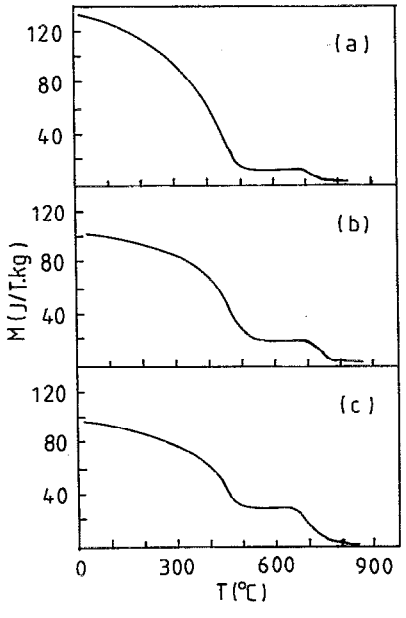

FIG. 2. Temperature dependence of magnetization in an applied field of 1.2 T: (a) $Sm_2Fe_{17}N_y$ nitride powder, (b) $Sm_2Fe_{17}N_y$ nitride powder ball milled for 6 h and explosion sintered $Sm_2Fe_{17}N_y$ magnet.

$Sm_2Fe_{17}N_y$ main phases have a Curie temperature of about 475 °C in all cases. This means the explosion sintering does not affect the intrinsic magnetic properties. The second stage in the curves represents the α-Fe impurity, of which the height indicates its relative quantity in the samples.

The demagnetization curve of the explosion sintered $Sm_2Fe_{17}N_y$ magnet at room temperature is shown in Fig. 3(a). The remanence equals $B_r=0.83$ T, the intrinsic coercivity is $\mu_0 H_c=0.57$ T, and the energy product is $(BH)_{max}=88$ kJ/m^3. Compared to the aligned sample made by fixing the ball-milled powder with wax [Fig. 3(b)], the explosion sintering sample has an improved rectangularity of the demagnetization curve, but its intrinsic coercivity decreases (from $\mu_0 H_c=0.86$ to 0.57 T). This may be attributed to the grain interactions of the compact magnet during explosion sintering. However, the α-Fe impurity and the other amorphous impurity (see Sec. III B) in the magnet might also affect the coercivity.

B. Microstructure (samples C, D, and E)

The sintered $Sm_2Fe_{17}N_y$ magnet was investigated by SEM and TEM. By the SEM observation (see Fig. 4), we found that the explosion sintered magnets with different average particle size powders are quite homogeneous and we did not find any impurity phase, such as α-Fe. By TEM observation, we found that there are two remarkably different areas in the sintered magnet. The main one has no visible contrast [Fig. 5(a)], which means that there are no defects in this phase. The TEM diffraction pattern confirms that this main phase is $Sm_2Fe_{17}N_y$ [Fig. 5(b)]. The other

Downloaded 10 Nov 2009 to 159.226.231.70. Redistribution subject to AIP license or copyright; see http://jap.aip.org/jap/copyright.jsp

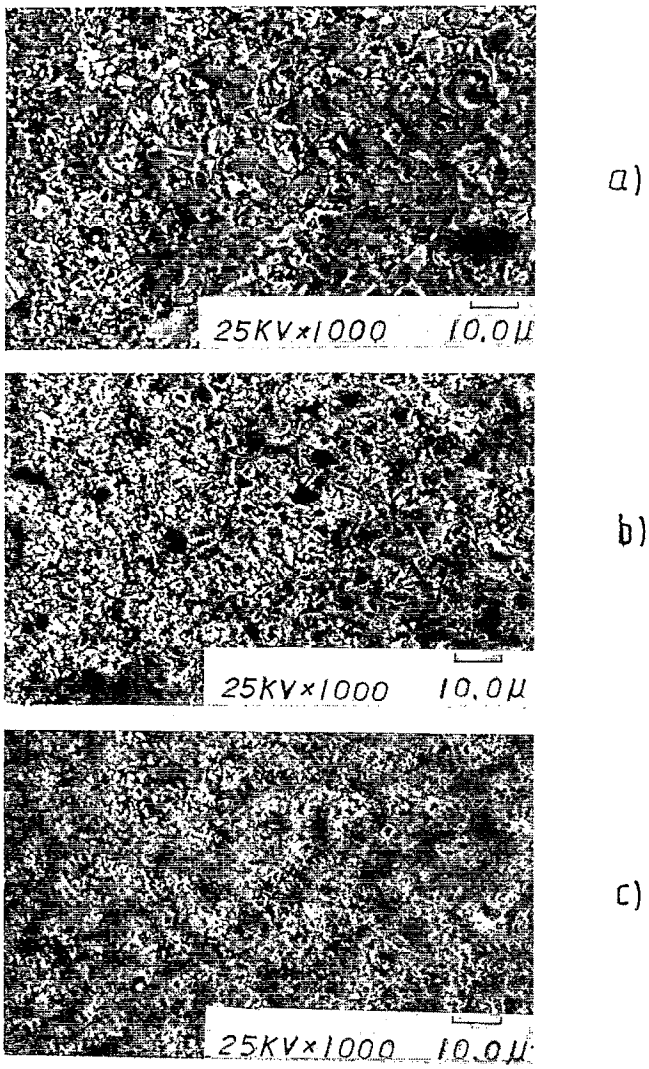

FIG. 4. SEM examination of the microstructure of sintered $Sm_2Fe_{17}N_y$ magnets with different average powder size $\langle\mu\rangle$: (a) $\langle\mu\rangle=5$ μm, (b) $\langle\mu\rangle=3$ μm, and (c) $\langle\mu\rangle=1$ μm.

minor one consists of tiny particles [Fig. 5(c)], the average sizes which are of the order of 0.1 μm. The TEM diffraction pattern shows that these particles are α-Fe and other unknown phases [Fig. 5(d)].

For both SEM and TEM observations, we did not find any grain-boundary phase, which indicates there are no pinning points in the sintered $Sm_2Fe_{17}N_y$ magnet.

C. Grain size dependence of coercivity (samples C, D, and E)

Figure 6 shows the demagnetization curves of ball-milled powder (before sintering) and the sintered magnets of the $Sm_2Fe_{17}N_y$ nitride. It can be seen that the intrinsic coercivity depends on the average size of the $Sm_2Fe_{17}N_y$ powder, especially before sintering. The nitride powder or sintered magnet with smaller average powder size has a higher coercivity. Also, the coercivity of sintered magnets decreases compared to that of their corresponding powder.

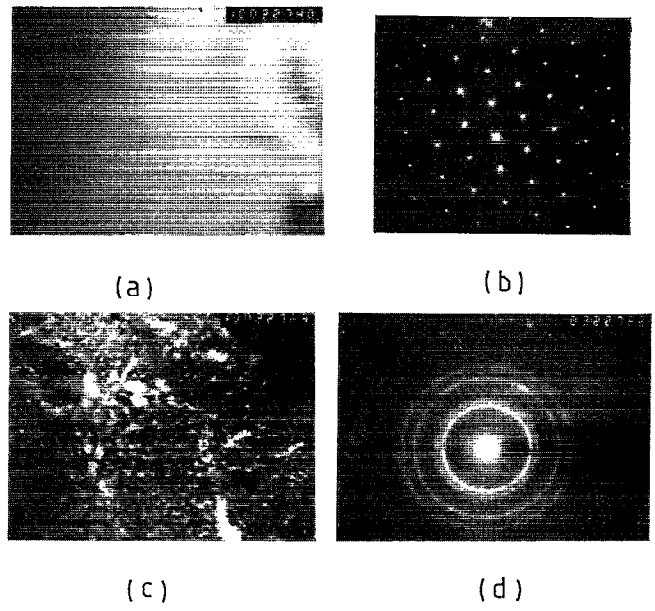

FIG. 5. Transmission electron micrograph of the sintered $Sm_2Fe_{17}N_y$ magnet: (a) $Sm_2Fe_{17}N_y$ grain without contrast, (b) diffraction pattern of $Sm_2Fe_{17}N_y$ grain along c axis, (c) the minor phase, and (d) diffraction pattern of the minor phase. For (a) and (c), the amplification is 10^5. For (b) and (d), $L\lambda=3.071$ cm Å.

D. Temperature dependence of coercivity (sample B)

The demagnetization curves of the sintered $Sm_2Fe_{17}N_y$ magnet as a function of temperature are shown in Fig. 7.

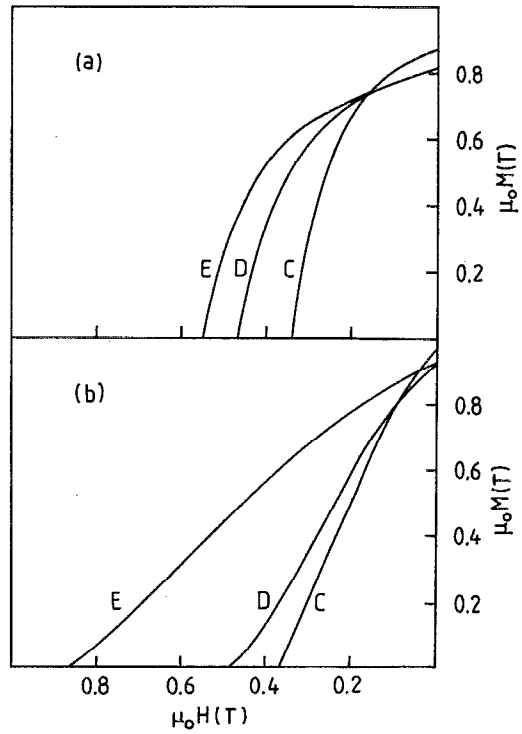

FIG. 6. Demagnetization curves of (a) sintered magnet of $Sm_2Fe_{17}N_y$ nitride and (b) ball milled powder (before sintering).

Downloaded 10 Nov 2009 to 159.226.231.70. Redistribution subject to AIP license or copyright; see http://jap.aip.org/jap/copyright.jsp

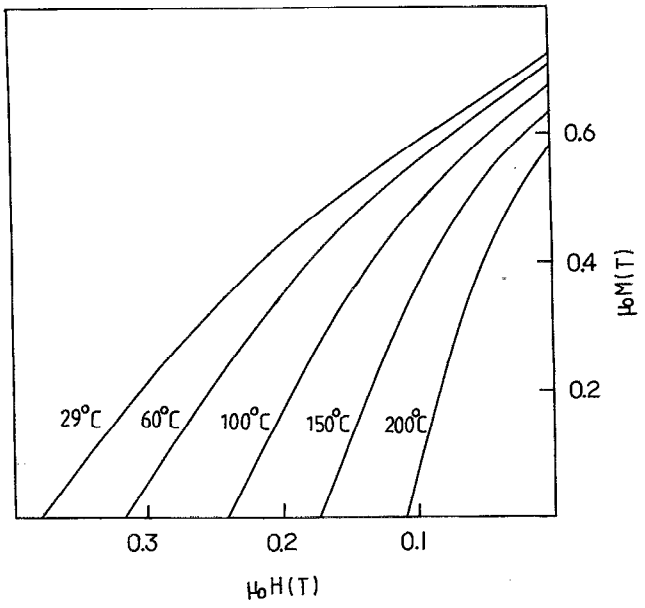

FIG. 7. Demagnetization curves of the sintered $Sm_2Fe_{17}N_y$ magnet as a function of temperature.

Both the remanence and the intrinsic coercivity decrease with temperature. The values in Table I are derived from Fig. 7, except for those of H_A and M_s, which are taken from Refs. 14 and 15, respectively.

Figure 8(a) compares the temperature dependence of coercivities of a sintered $Sm_2Fe_{17}N_y$ magnet and a $Nd_{15}Fe_{77}B_8$ magnet.[16] The data are normalized by that at room temperature. It can be seen that, with increasing temperature, the coercivity of the $Sm_2Fe_{17}N_y$ magnet decreases more slowly than that of the $Nd_{15}Fe_{77}B_8$ magnet.

When studying the coercivity of sintered Nd-Fe-B magnets, Krönmuller *et al.* proposed a model to describe the mechanism.[17,18] Since there are no defects in the $Nd_2Fe_{14}B$ main phase, the nucleations are located at the inhomogeneous layer of the main phase grains. Considering the grain misalignment and the local demagnetizing field, we obtain the following relationship:

$$H_N = cH_A - N_{\text{eff}}M_s, \tag{1}$$

where H_N is the nucleation field, (i.e., the theoretic value of ${}_iH_c$) and N_{eff} is the effective demagnetization factor. H_A and M_s are the anisotropy field and saturation magnetization of $Nd_2Fe_{14}B$, respectively, which are only dependent on temperature. The constant c is related to the alignment of grains, the decoupling of grains, and the thickness and magnetic properties of the inhomogeneous layer of a grain. Qualitatively speaking, the worse the alignment, the thicker the inhomogeneous layer; the larger the difference in the magnetic properties between the layer and the main phase, the smaller the c value. Both c and N_{eff} are independent of temperature.

TABLE I. Magnetic properties of sintered $Sm_2Fe_{17}N_y$ magnet at different temperatures (values of μ_0H_A are taken from Ref. 4).

T (°C)	29	60	100	150	200
B_r (T)	0.725	0.712	0.680	0.640	0.584
$\mu_0{}_iH_c$ (T)	0.380	0.318	0.243	0.175	0.110
$B_r/B_r(20\,°C)$	1	0.982	0.938	0.883	0.806
${}_iH_c/{}_iH_c(20\,°C)$	1	0.837	0.639	0.461	0.289
μ_0M_s (T)	1.33	1.29	1.26	1.19	1.12
μ_0H_A (T)	13.6	12.4	10.7	9.1	7.7
H_A/M_s	10.3	9.59	8.48	7.67	6.86
${}_iH_c/M_s$	0.286	0.246	0.193	0.148	0.098

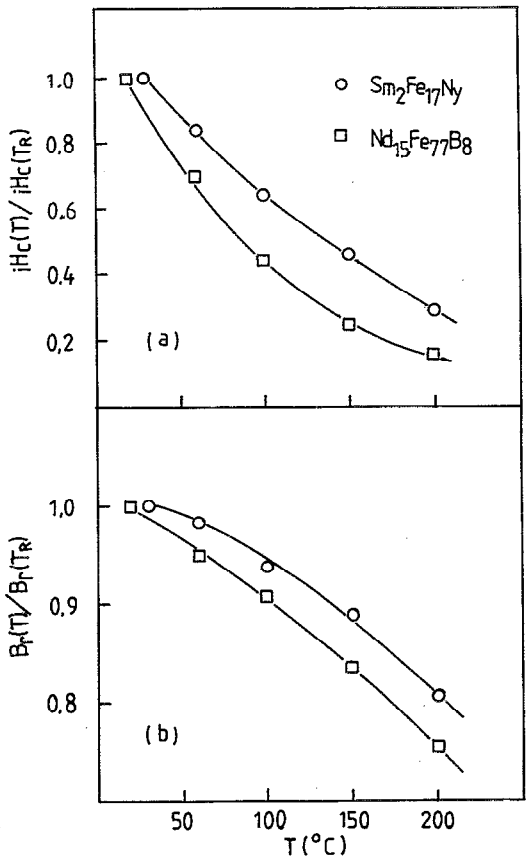

FIG. 8. Temperature dependence of (a) coercive field and (b) the remanence B_r of the sintered $Sm_2Fe_{17}N_y$ magnet, compared with those of the $Nd_{15}Fe_{77}B_8$ magnet.

We now extend this model to the coercivity study of the $Sm_2Fe_{17}N_y$ nitride. Since there is no defect inside the grain and no boundary phase between the grains, the nucleations of the ball-milled powder and explosion sintered magnet of $Sm_2Fe_{17}N_y$ nitride both could be attributed to the inhomogeneous layer of the $Sm_2Fe_{17}N_y$ grains. Plotting ${}_iH_c/M_s$ vs H_A/M_s at different temperature by the values in Table I (see Fig. 9), we can see that formula (1) holds very well. From the linear relationship we can obtain c and N_{eff} by the slope and the intercept. For a comparison, the corresponding values (see Table II) of $Nd_{15}Fe_{77}B_8$ are also plotted in Fig. 8. From Fig. 9 we derived that c(SmFeN) $=0.054$ and N_{eff}(SmFeN) $=0.27$ compared to c(NdFeB) $=0.35$ and N_{eff}(NdFeB) $=1.0$. Using these figures we estimated the thickness of the inhomogeneous layer is of an order of 10^2 Å.[16,17] With decreasing size of the $Sm_2Fe_{17}N_y$

Downloaded 10 Nov 2009 to 159.226.231.70. Redistribution subject to AIP license or copyright; see http://jap.aip.org/jap/copyright.jsp

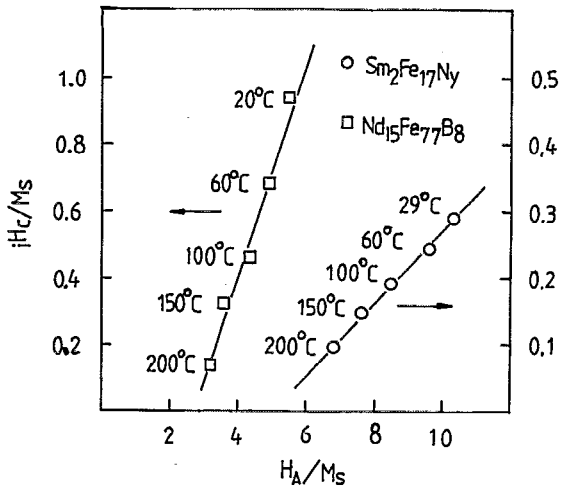

FIG. 9. $_iH_c/M_s$ vs H_A/M_s plot for the sintered $Sm_2Fe_{17}N_y$ magnet, compared with that for the $Nd_{15}Fe_{77}B_8$ magnet.

powder, the nucleation on the surface layer becomes harder. Therefore, the coercivity increases. When the particle size is too small, the oxidation may destroy the coercivity.

E. Temperature coefficient (sample B)

Figure 8(b) gives the temperature dependence of the remanence B_r of the sintered $Sm_2Fe_{17}N_y$ magnet, compared with that of the Nd-Fe-B magnet.[14] It can be seen that the B_r of the former decreases more slowly than the latter.

The temperature coefficients α of B_r and β of $_iH_c$ in a temperature range T_1–T_2 are defined as

$$\alpha=[B_r(T_2)-B_r(T_1)]/[(T_2-T_1)B_r(T_1)], \quad (2)$$

$$\beta=[{}_iH_c(T_2)-{}_iH_c(T_1)]/[(T_2-T_1)/{}_iH_c(T_1)]. \quad (3)$$

Using the data in Tables I and II, and choosing T_1 as room temperature, and using formulas (2) and (3), we derived the temperature coefficients α and β of sintered $Sm_2Fe_{17}N_y$ and Nd-Fe-B, respectively, at different temperatures (see Table III and Fig. 10). Combining the features of Figs. 8(a) and 8(b), we may conclude that the sintered $Sm_2Fe_{17}N_y$ magnet has a better thermal stability than the $Nd_2Fe_{14}B$ magnet.

TABLE II. Magnetic properties of $Nd_{15}Fe_{77}B_8$ magnet (N-35) at different temperatures (data are taken from Ref. 16 except μ_0M_s from Ref. 19 and μ_0H_A from Ref. 20).

T (°C)	20	60	100	150	200
B_r (T)	1.22	1.16	1.11	1.02	0.92
$\mu_0\,{}_iH_c$ (T)	1.51	1.05	0.66	0.37	0.16
B_r/B_r(20 °C)	1	0.951	0.910	0.836	0.754
$_iH_c/{}_iH_c$(20 °C)	1	0.695	0.437	0.245	0.156
μ_0M_s (T)	1.60	1.54	1.43	1.35	1.19
μ_0H_A (T)	8.80	7.65	6.29	4.88	3.88
H_A/M_s	5.50	4.97	4.40	3.62	3.26
$_iH_c/M_s$	0.944	0.682	0.462	0.274	0.134

TABLE III. The temperature coefficients α of B_r and β of $_iH_c$ of sintered $Sm_2Fe_{17}N_y$ magnet at different temperatures, compared with those of the $Nd_{15}Fe_{77}B_8$ magnet (N-35) of which data are taken from Ref. 16.

T (°C)	29	60	100	150	200
α_{SmFeN} (%/°C)	···	−0.058	−0.076	−0.097	−0.114
β_{SmFeN} (%/°C)	···	−0.53	−0.51	−0.45	−0.42
T (°C)	20	60	100	150	200
α_{NdFeB} (%/°C)	···	−0.123	−0.113	−0.126	−0.137
β_{NdFeB} (%/°C)	···	−0.761	−0.704	−0.580	−0.497

IV. CONCLUSION

As a new technique, explosion sintering has been successfully used to make compact magnets from $Sm_2Fe_{17}N_y$ powder, which retains the crystalline structural, and magnetic properties of the $Sm_2Fe_{17}N_y$ nitride. Compared to the epoxy resin bonded $Sm_2Fe_{17}N_y$ magnet, the explosion sintered $Sm_2Fe_{17}N_y$ magnet has better rectangularity of the demagnetization curve to get a higher energy product. The coercivity of the $Sm_2Fe_{17}N_y$ nitride magnet, as well as the powder, may originate from the nucleation in the grain surface layer. The $Sm_2Fe_{17}N_y$ magnets have better temperature coefficients than the Nd-Fe-B magnets.

ACKNOWLEDGMENT

This work was partly supported by the National Science Foundation of China and Magnetism Laboratory, Institute of Physics, Chinese Academy of Sciences.

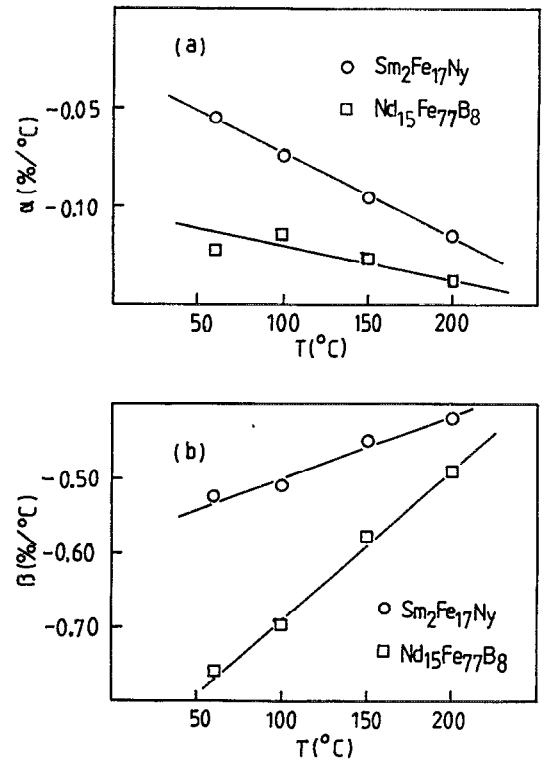

FIG. 10. Variation of temperature coefficient α and β of sintered $Sm_2Fe_{17}N_y$ magnet, compared with those of the $Nd_{15}Fe_{77}B_8$ magnet.

Downloaded 10 Nov 2009 to 159.226.231.70. Redistribution subject to AIP license or copyright; see http://jap.aip.org/jap/copyright.jsp

[1] J. M. D. Coey and H. Sun, J. Magn. Magn. Mater. **87**, L251 (1990).
[2] H. Sun, J. M. D. Coey, Y. Otani, and D. P. F. Hurley, J. Condensed Mater. **2**, 6465 (1990).
[3] K. H. J. Buschow, R. Coehoorn, D. B. de Mooij, K. de Waard, and T. H. Jacobs, J. Magn. Magn. Mater. **92**, L35 (1990).
[4] M. Katter, J. Wecker, L. Schultz, and R. Grössinger, J. Magn. Magn. Mater. **92**, L14 (1990).
[5] B.-P. Hu, H.-S. Li, H. Sun, and J. M. D. Coey, J. Condensed Mater. **3**, 3983 (1991).
[6] S. S. Jaswal, W. B. Yelon, G. C. Hadjipanayis, Y. Z. Wang, and D. J. Sellmyer, Phys. Rev. Lett. **67**, 644 (1991).
[7] H.-S. Li and J. M. Cadogan, J. Magn. Magn. Mater. **103**, 53 (1992).
[8] K. Schnitzke, L. Schultz, J. Wecker, and M. Katter, Appl. Phys. Lett. **57**, 2853 (1990).
[9] Y. Otani, A. Moukarika, H. Sun, and J. M. D. Coey, J. Appl. Phys. **69**, 5585 (1991).
[10] M. Q. Huang, L. Y. Zhang, B. M. Ma, Y. Zheng, J. Elbicki, S. G. Sankar, and W. E. Wallace, J. Appl. Phys. **70**, 6027 (1991).
[11] Y.-L. Liu, D.-W. Wang, B.-P. Hu, J.-L. Gao, Q. Song, L. Liu, X.-L. Rao, J.-M. Xu, G.-C. Liu, F. Cao, H. Li, L. Yin, N. Tang, M.-J. Yu, Tergus, and Z.-X. Wang, Kexue Tongbao **36**, 1850 (1991).
[12] Z.-D. Zhang (private communication).
[13] J.-M. Xu, B.-P. Hu, X.-L. Rao, G.-Ch. Liu, X.-L. Dong, Y.-L. Liu, D.-W. Wang, J.-L. Gao, F. Cao, Y.-Z. Wang, Q. Song, L. Liu, Z.-X. Wang, D.-X. Zhang, M. Cai, S.-H. Li, H. Li, and L. Yin, Kexue Tongbao **37**, 1462 (1992).
[14] S. Miraglia, J. L. Soubeyroux, C. Kolbeck, O. Isnard, D. Fruchart, and M. Guillot, J. Less-Common Metals **71**, 51 (1991).
[15] B.-P. Hu, X.-L. Rao, J.-M. Xu, G.-C. Liu, F. Cao, and X.-L. Dong, J. Magn. Magn. Mater. **114**, 138 (1992).
[16] D. Li, H. F. Mildrum, and K. J. Strnat, J. Appl. Phys. **57**, 4140 (1985).
[17] H. Krönmuller, K.-D. Durst, and G. Martinek, J. Magn. Magn. Mater. **69**, 149 (1987).
[18] H. Krönmuller, K.-D. Durst, S. Hock, and G. Martinek, J. Phys. (Paris) **49**, C8-623 (1988).
[19] S. Hirosama, Y. Matsnura, H. Yamamoto, S. Fujimura, M. Sagawa, and H. Yamauchi, J. Appl. Phys. **59**, 873 (1986).
[20] K.-D. Durst and H. Kronmuller, J. Magn. Magn. Mater. **59**, 86 (1986).

Downloaded 10 Nov 2009 to 159.226.231.70. Redistribution subject to AIP license or copyright; see http://jap.aip.org/jap/copyright.jsp